Understanding Spin Structure in Metallacrown Single-Molecule Magnets using Magnetic Compton Scattering

ARTICLE *in* JOURNAL OF THE AMERICAN CHEMICAL SOCIETY · MARCH 2014

Impact Factor: 12.11 · DOI: 10.1021/ja501452w · Source: PubMed

JACS
JOURNAL OF THE AMERICAN CHEMICAL SOCIETY
Communication
pubs.acs.org/JACS

Understanding Spin Structure in Metallacrown Single-Molecule Magnets using Magnetic Compton Scattering

Aniruddha Deb,[†] Thaddeus T. Boron, III,[†,#] Masayoshi Itou,[‡] Yoshiharu Sakurai,[‡] Talal Mallah,[§] Vincent L. Pecoraro,[†] and James E. Penner-Hahn*[,†,⊥]

[†]Department of Chemistry, University of Michigan, Ann Arbor, Michigan 48109, United States
[⊥]Program in Biophysics, University of Michigan, Ann Arbor, Michigan 48109, United States
[‡]Japan Synchrotron Radiation Research Institute (JASRI)/SPring-8, Sayo, Hyogo 679-5198, Japan
[§]Institut de Chimie Moléculaire et des Matériaux d'Orsay, CNRS, Université de Paris Sud, 91405 Orsay Cedex, France

Supporting Information

ABSTRACT: The 3d−4f mixed metallacrowns frequently show single-molecule magnetic behavior. We have used magnetic Compton scattering to characterize the spin structure and orbital interactions in three isostructural metallacrowns: Gd_2Mn_4, Dy_2Mn_4, and Y_2Mn_4. These data allow the direct determination of the spin only contribution to the overall magnetic moment. We find that the lanthanide 4f spin in Gd_2Mn_4 and Dy_2Mn_4 is aligned parallel to the Mn 3d spin. For Y_2Mn_4 (manganese-only spin) we find evidence for spin delocalization into the O 2p orbitals. Comparing the magnetic Compton scattering data with SQUID studies that measure the total magnetic moment suggests that Gd_2Mn_4 and Y_2Mn_4 have only a small orbital contribution to the moment. In contrast, the total magnetic moment for Dy_2Mn_4 MCs is much larger than the spin-only moment, demonstrating a significant orbital contribution to the overall magnetic moment. Overall, these data provide direct insight into the correlation of molecular design with molecular magnetic properties.

The discovery of single-molecule magnets (SMMs) in polynuclear complexes, where the exchange coupling between magnetic metal ions leads to a high-spin ground state and an Ising-type magnetic anisotropy responsible for their magnetic bistability, has fostered intense interest in understanding the complex magnetic properties of these materials.[1] On the practical level, SMMs and magnetic materials have the potential to be used as building blocks for information storage and quantum information processing, spintronics, and magnetocaloric refrigeration.[2−5]

The first SMMs to be described were based on multinuclear Mn complexes.[6−12] Recent examples have been found based on other 3d, 4d, and 5d transition-metal ions as well as SMMs based on the combination of 3d and 4f ions.[13−19] Such systems typically maximize the total spin of the ground state, S_T, while retaining an Ising-type anisotropy (negative zero field splitting parameter, D, corresponding to the spin Hamiltonian $H = D[S_z^2 - S(S+1)/3]$, so that when D is negative, the ground-state sublevel is the one with the largest M_S value), since the energy barrier for relaxation is related to S_T^2 and $|D|$. Unfortunately, for polynuclear complexes with a large spin ground state S_T, the $|D|$ value is found to be small so that the large spin of the ground state hardly compensates the weak overall magnetic anisotropy. We have been exploring methods to enhance magnetoanisotropy using metallacrowns (MCs) as SMMs.[20−22] The MCs are inorganic analogues of crown ethers, and we have found that when Mn-based MCs bind 4f-elements, they frequently show SMM properties. The presence of Jahn−Teller distorted Mn^{III} ions combined with lanthanide ions having strong spin−orbital coupling may lead to high magnetic anisotropy. Mixed d−f orbital SMMs can enhance the anisotropic component necessary for slow magnetic relaxation if there is sizable exchange coupling between the lanthanides and the transition-metal ions; this in turn depends on the degree of spin delocalization (covalency) from the metal to the surroundings ligands.

One example of mixed d−f orbital SMMs is the family of complexes $[Ln^{III}(O_2CCH_3)(NO_3)_2$ 14-$MC_{Mn(III)Ln(III)(\mu\text{-}O)(\mu\text{-}OH)N(shi)}-5]\cdot 3C_3H_7NO\cdot 7C_5H_5N\cdot H_2O$ [where shi = salicylhydroximate^{3-} and Ln = Y^{III}, Gd^{III}, Tb^{III}, Dy^{III}, and Ho^{III}].[23] The structural topology includes oxime N−O bridges between all Mn atoms and between two of the Mn atoms and a Ln(III) that forms part of the MC ring (this Ln(III) is designated $Ln(III)_{out}$). There are also μ_3-O and μ_2-OH bridges between two of the Mn^{III} ions. Finally, there are four Mn-O-$Ln(III)_{in}$ single atom bridges (originating from an oxime linkage) between the Mn^{III} atoms that make the metallacrown ring and the Ln(III) that is captured in the MC cavity, which is designated $Ln(III)_{in}$ (see Figure S1). The spin arrangement in these systems results in a large magnetic moment and SMM behavior for the Tb^{III}, Ho^{III} and Dy^{III} systems with an effective energy barrier of 16.7 cm^{-1} for the Dy_2Mn_4 complex. In order to understand the spin structure and magnetic properties of these complexes better and to unravel the role of the spin and orbital angular momentum to the total magnetic moment, we have undertaken a series of magnetic Compton scattering measurements of both the SMM materials and a reference complex with unpaired spin only on the transition-metal ions. Magnetic Compton scattering (MCS) permits direct interrogation of the spin-polarized orbitals in

Received: February 11, 2014
Published: March 13, 2014

   dx.doi.org/10.1021/ja501452w | J. Am. Chem. Soc. 2014, 136, 4889−4892

magnetic systems.[24−27] X-ray magnetic circular dichroism (XMCD) provides complementary information; it permits element specific measurements but does not allow a direct measurement of the spin moment.[28,29] To our knowledge, the present work is the first application of MCS to molecular materials.

Compton scattering results from the interaction of an incident X-ray with an electron and thus provides a direct probe of the electron distribution in a sample. The Compton profile, $J(p_z)$, can be calculated from the integrated ground-state electron momentum density as

$$J(p_z) = \int\int \left(\sum_i |\rho_{i\uparrow}(\mathbf{p})|^2 + \sum_i |\rho_{i\downarrow}(\mathbf{p})|^2\right) dp_x dp_y \quad (1)$$

If the sample has a magnetic moment and incident X-rays are circularly polarized the Compton profile will depend on the orientation of an applied field. The magnetic Compton profile (MCP), $J_{mag}(p_z)$, is defined as the field-dependent differential scattering:

$$J_{mag}(p_z) = \int\int \left(\sum_i |\rho_{i\uparrow}(\mathbf{p})|^2 - \sum_i |\rho_{i\downarrow}(\mathbf{p})|^2\right) dp_x dp_y \quad (2)$$

where the spin-up and -down electron momentum densities are represented by $\rho_{i\uparrow}(\mathbf{p})$ and $\rho_{i\downarrow}(\mathbf{p})$, respectively, and i runs over the occupied electronic states, with the z-component of the electron momentum, p_z, chosen to lie along the direction of the scattering vector. If a circularly polarized X-ray beam is used, the Compton scattering will depend on $J_{mag}(p_z)$. The MCP can thus be measured by determining the change in scattering either as the polarization is switched from left- to right-circularly polarized with a fixed field or as the magnetic field is switched with a fixed polarization; in practice the latter is experimentally more tractable. The flipping ratio R_{sample}, which is proportional to the MCP, is defined as

$$R_{sample} = \frac{I^+ - I^-}{I^+ + I^-} \propto \frac{\int J_{mag}(p_z) dp_z}{\int J(p_z) dp_z} \quad (3)$$

where I^+ and I^- are the intensities of Compton-scattered X-rays with different magnetization directions.

The area under the MCP is directly proportional to the spin moment of the sample. Therefore, by comparing the MCP for an unknown with the MCP of a known material, the spin-only moment of a sample, μ_{sample}, can be determined. We compared R_{sample} to R_{Fe}, the flipping ratio for Fe measured under the same experimental conditions. If M_{sample} and M_{Fe} are defined as the effective number of electrons contributing to the total inelastic scattering for the sample and for Fe, respectively, then

$$\mu_{sample} = \mu_{Fe}\left(\frac{M_{sample}R_{sample}}{M_{Fe}R_{Fe}}\right) \quad (4)$$

Since the spin moment for Fe is well-known (2.1 μ_B),[30] eq 4 allows direct determination of the spin-only portion of the magnetic moment for a sample.

In addition to providing the spin moment, the MCP is also sensitive to the details of the electronic structure. Since the shape of the Compton profile is different for each orbital, we are able to determine the relative contributions of p-, d- (e_g and t_{2g}), and f-orbitals to the spin magnetic moment. Within the impulse approximation, the MCP is sensitive only to the spin magnetic moment, S and not to the orbital moment L.[31,32] Unlike XMCD, MCPs are equally sensitive to all spin polarized electrons, regardless of their binding energy and the symmetry of their wave functions.

The MCP of Gd_2Mn_4 is shown in Figure 1 and that for Dy_2Mn_4 in Figure S2. For both complexes the MCP is quite

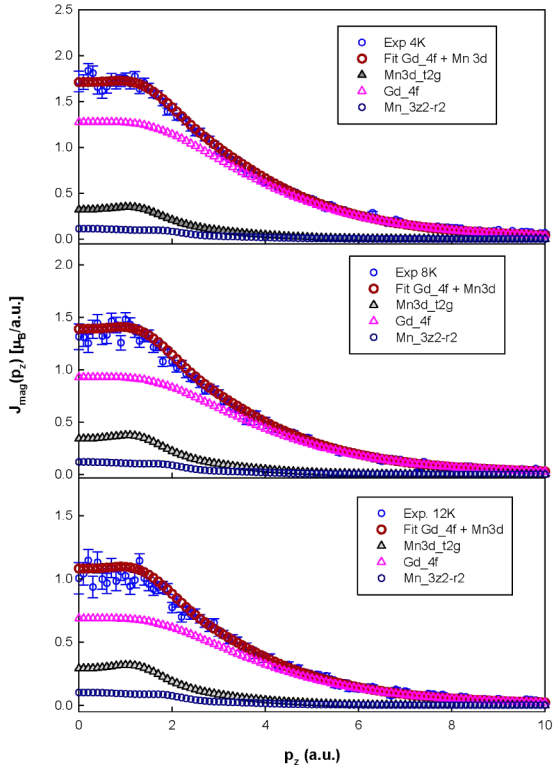

Figure 1. Individual orbital-wise contributions of Gd-4f, and Mn-3d (t_{2g} and e_g) for Gd_2Mn_4 at 4, 8, and 12 K.

broad, reflecting the significant 4f contribution. However, in both cases, the MCP could only be fit by including contributions from both 4f and 3d (both t_{2g} and e_g). Although the t_{2g} and the e_g components of the 3d MCPs were allowed to refine independently, the observed best fits gave the expected 3:1 ratio of t_{2g}:e_g spin for a high-spin Mn^{III}. The quantitative fitting results at each measured temperature are given in Table 1. As expected, the magnetic character of each complex is dominated by the Ln-4f orbitals.

The MCP for Y_2Mn_4 is shown in Figure 2. The profile here is noticeably narrower, as expected given the absence of unpaired f-electrons in Y^{III}. Although the MCP is dominated by Mn 3d components, it was not possible to obtain a good fit to the detailed shape at low p_z without including a small amount of oxygen 2p scattering. This provides direct evidence for spin delocalization into the oxygen 2p orbitals or spin polarization of Mn 3d−O 2p hybridized orbitals. In total, as many as 24 different oxygen orbitals could contribute to the observed MCP, and from the present isotropic MCP data it is only possible to determine that the *net* O 2p unpaired spin contribution in Y_2Mn_4 is nonzero. It is likely that the dominance of the 4f contributions, accounts for the absence of detectable 2p signals for Gd_2Mn_4 and Dy_2Mn_4.

For Y_2Mn_4, the Y^{III} is diamagnetic, and all the magnetic contributions come from the Mn 3d orbitals. For an isolated high-spin Mn^{III}, the magnetic moment at 4 K and 2.5 T is very close to 4 μ_B, or, if the Mn were noninteracting, 16 μ_B/formula

dx.doi.org/10.1021/ja501452w | J. Am. Chem. Soc. 2014, 136, 4889−4892

Table 1. Temperature-Dependent Orbital-Decomposed Magnetic Moments[a] Determined From MCPs

	temp, K	μ_{spin}	Dy 4f	Gd 4f	Mn 3d t_{2g}	Mn 3d $3z^2-r^2$	O 2p	μ_{total}[b]
Y_2Mn_4	4	3.29			2.40	0.8	0.1	2.4
	9	2.90			2.04	0.68	0.2	
Gd_2Mn_4	4	13.37		10.98	1.79	0.6		14.3
	8	10.54		7.98	1.90	0.63		
	12	8.10		5.91	1.63	0.54		
Dy_2Mn_4	7	4.12	3.45		0.49	0.16		12.1 at 5 K
	10	3.78	2.99		0.58	0.19		

[a]All magnetic moment values are given in Bohr magnetons per formula unit. [b]Total magnetic moment from SQUID magnetization studies.

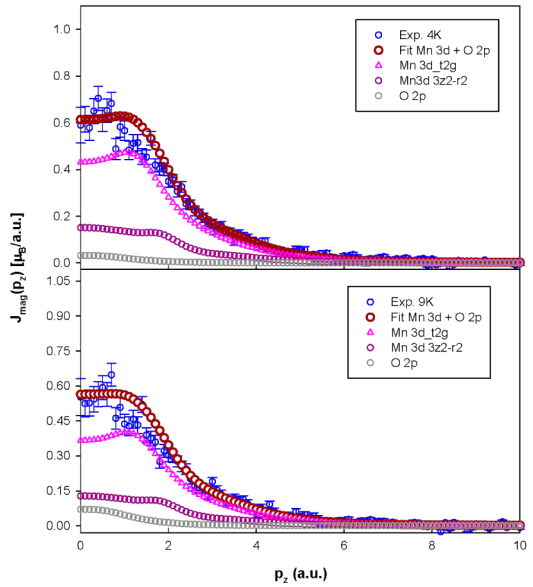

Figure 2. Individual orbital-wise contributions of Mn-3d (t_{2g} and e_g) and delocalized O-2p for Y_2Mn_4 at 4 and 9 K.

unit. This is considerably larger than the observed SQUID (2.4 μ_B) and MCP (3.3 μ_B) values, indicating the presence of significant antiferromagnetic exchange coupling in this complex. The fit of the magnetic data of the Y_2Mn_4 complex (see SI) shows that the ground spin state is $S = 0$, but there are three low-lying spin states namely $S = 1$, 2, 3, and 4 within 5 cm^{-1} that contribute to the magnetic moment at $T = 5$ K and $H = 2.5$ T. While it is expected that high-spin Mn^{III} complexes will show appreciable spin orbit coupling ($|D| \sim 2-4$ cm^{-1}), the close correspondence of μ_{spin} and μ_{total} for this system shows that there is only a small orbital contribution to the magnetic moment indicating that the total molecular anisotropy is small.

This observation is quite interesting for evaluating synthetic strategies for preparing SMMs. One approach to the design of SMMs is to geometrically restrict each of the Mn^{III} ions within a planar topology in order to compel parallel alignment of the easy axes of each Mn ion and thus optimize the Ising-type magnetoanisotropy of the system. By using MCP, one can directly evaluate this strategy by subtracting the spin component to arrive at the orbital contribution to the magnetism. One can see for this example that despite achieving the desired rigorous planarity of the four Mn^{III} ions, the Ising-type anisotropy apparently still is not additive. Thus, MCP represents an exciting way to probe the efficacy of architectural control for the development of molecular magnets.

Comparison of the fitted MCP results with the total moment determined by SQUID (Table 1) shows that the MCP spin-only moment for Gd_2Mn_4 (13.4 μ_B) is very close to the magnetic moment obtained by SQUID (14.3 μ_B). This confirms again that there is little or no orbital contribution to the magnetic moment in this complex. The spin magnetic moment on Gd at 4 K (11 μ_B, see Table 1) is within the range corresponding to uncoupled or very weakly coupled moments (see Figure S5). A schematic representation of the Gd_2Mn_4 magnetic interactions is shown in Figure 3. The Gd^{III}_{in} ion

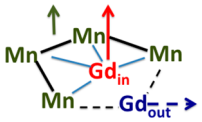

Figure 3. Interpretation of magnetization of the individual spin-component of Gd and Mn in the Gd_2Mn_4 MC system. The red and green arrows illustrate the ferromagnetic alignment of the combined moment of the Mn ions and the inner Gd ion (Gd_{in}), while the dashed blue arrow indicates that the outer Gd (Gd_{out}) remains uncoupled or is only weakly coupled to the Mn and Gd spins.

(red) is connected to the 4 Mn^{III} atoms (green) by single oxygen atoms (Figure 3), while the metallacrown ring Gd ion (Gd_{out}) is connected by two 2-atom (O−N) bridges. The inner Gd−Mn coupling interaction (represented by light-blue lines) most likely dominates the total Gd^{III}−Mn^{III} exchange, and thus the outer Gd ion contribution can reasonably be neglected (represented by dashed lines). The solid black lines represent the direct Mn−Mn exchange interactions. Enhancement of the exchange coupling between the Mn^{III} ions can be attributed to their interaction with the inner Gd^{III} ion. This is represented by the red and green vectors in Figure 3. An interesting result is that the sign of the spin densities on Gd_{in} and the Mn ions is the same. This can be explained as the result of a ferromagnetic exchange coupling between Gd_{in} and the Mn^{III} ions. This ferromagnetic coupling competes with the weak antiferromagnetic coupling between the Mn1 ions on the one hand and the Mn2 ions on the other (see Figure S1) and thus leads to an overall moment on Mn aligned with that of Gd_{in}.

The behavior of Dy_2Mn_4 is quite different from that of the isostructural Gd_2Mn_4 complex. The spin-only moment is dominated by the Dy, and the Mn spin-only moment is significantly smaller than in Gd_2Mn_4. In contrast with Y_2Mn_4 and Gd_2Mn_4, the total magnetic moment for Dy_2Mn_4 is significantly larger than the spin-only moment, presumably as a result of Dy orbital magnetic moment.

In summary, MCP measurements have allowed, for the first time, the direct separation of spin and orbital contributions to the total magnetic moment in metallacrown SMM materials, allowing us to test whether structural alignment of Ising-type ions maximizes the orbital contribution to the magnetic moments within the system. These measurements are the first application of MCP to molecular materials. These data

dx.doi.org/10.1021/ja501452w | J. Am. Chem. Soc. 2014, 136, 4889−4892

confirm the expected 3:1 ratio of t_{2g}:e_g electrons in Mn and demonstrate that there is little orbital magnetism from the Mn. We find that the total magnetic moment in the Dy complex is dominated by orbital contributions, and comparison of the data for Dy_2Mn_4 and Y_2Mn_4 suggests that there is significant Dy−Mn spin coupling in the former. Finally, these data provide direct evidence for Mn−O covalency.

■ ASSOCIATED CONTENT

Supporting Information

Schematic illustration of MC connectivities, experimental details, alternate fits using different combinations of p, d, and f orbitals, fits of the SQUID data for Y_2Mn_4 and magnetization of two Gd(III) ions with different values of the coupling parameters 2*J*. This material is available free of charge via the Internet at http://pubs.acs.org.

■ AUTHOR INFORMATION

Corresponding Author

jeph@umich.edu

Present Address

[#]Department of Chemistry, Slippery Rock University, Slippery Rock, PA 16057, United States.

Notes

The authors declare no competing financial interest.

■ ACKNOWLEDGMENTS

This research was supported in part by the National Science Foundation under grant CHE-1057331 (V.P.) and was carried out under the framework for the European Union IRSES Project Metallacrowns-Metallacrowns-based innovative materials and supramolecular devices. This work was performed with approval from JASRI/SPring-8, Japan proposal nos. 2011B1173, 2012A1051, 2013A1069. The authors thanks the Fondation de l'Ecole Normale and the Region Ile de France for the Blaise Pascal Chair of Pr. V.P.

■ REFERENCES

(1) *Single-Molecule Magnets and Related Phenomena*, Structure and Bonding Series; Winpenny, R., Ed.; Springer: New York, 2006; Vol. *122*.

(2) Leuenberger, M. N.; Loss, D. *Nature* **2001**, *410*, 789.

(3) Milios, C. J.; Vinslava, A.; Wernsdorfer, W.; Moggach, S.; Parsons, S.; Perlepes, S. P.; Christou, G.; Brechin, E. K. *J. Am. Chem. Soc.* **2007**, *129*, 2754.

(4) Affronte, M.; Casson, I.; Evangelisti, M.; Candini, A.; Carretta, S.; Muryn, C.; Teat, S. J.; Timco, G. A.; Wernsdorfer, W.; Winpenny, R. E. P. *Angew. Chem., Int. Ed.* **2005**, *44*, 6496.

(5) Bogani, L.; Wernsdorfer, W. *Nat. Mater.* **2008**, *7*, 179.

(6) Hill, S.; Murugesu, M.; Christou, G. *Phys Rev B* **2009**, *80*, 174416.

(7) Chakov, N. E.; Soler, M.; Wernsdorfer, W.; Abboud, K. A.; Christou, G. *Inorg. Chem.* **2005**, *44*, 5304.

(8) Cornia, A.; Sessoli, R.; Sorace, L.; Gatteschi, D.; Barra, A. L.; Daiguebonne, C. *Phys. Rev. Lett.* **2002**, *89*, 257201.

(9) Aubin, S. M.; Sun, Z.; Eppley, H. J.; Rumberger, E. M.; Guzei, I. A.; Folting, K.; Gantzel, P. K.; Rheingold, A. L.; Christou, G.; Hendrickson, D. N. *Inorg. Chem.* **2001**, *40*, 2127.

(10) Inglis, R.; White, F.; Piligkos, S.; Wernsdorfer, W.; Brechin, E. K.; Papaefstathiou, G. S. *Chem. Commun. (Cambridge, U. K.)* **2011**, *47*, 3090.

(11) Langley, S. K.; Stott, R. A.; Chilton, N. F.; Moubaraki, B.; Murray, K. S. *Chem. Commun. (Cambridge, U. K.)* **2011**, *47*, 6281.

(12) Milios, C. J.; Inglis, R.; Vinslava, A.; Bagai, R.; Wernsdorfer, W.; Parsons, S.; Perlepes, S. P.; Christou, G.; Brechin, E. K. *J. Am. Chem. Soc.* **2007**, *129*, 12505.

(13) Osa, S.; Kido, T.; Matsumoto, N.; Re, N.; Pochaba, A.; Mrozinski, J. *J. Am. Chem. Soc.* **2004**, *126*, 420.

(14) Zaleski, C. M.; Depperman, E. C.; Kampf, J. W.; Kirk, M. L.; Pecoraro, V. L. *Angew. Chem., Int. Ed. Engl.* **2004**, *43*, 3912.

(15) Zaleski, C. M.; Tricard, S.; Depperman, E. C.; Wernsdorfer, W.; Mallah, T.; Kirk, M. L.; Pecoraro, V. L. *Inorg. Chem.* **2011**, *50*, 11348.

(16) Guedes, G. P.; Soriano, S.; Mercante, L. A.; Speziali, N. L.; Novak, M. A.; Andruh, M.; Vaz, M. G. F. *Inorg. Chem.* **2013**, *52*, 8309.

(17) Iasco, O.; Novitchi, G.; Jeanneau, E.; Luneau, D. *Inorg. Chem.* **2013**, *52*, 8723.

(18) Abtab, S. M.; Majee, M. C.; Maity, M.; Titis, J.; Boca, R.; Chaudhury, M. *Inorg Chem* **2014**, *53*, 1295.

(19) Prasad, T. K.; Rajasekharan, M. V.; Costes, J. P. *Angew. Chem., Int. Ed.* **2007**, *46*, 2851.

(20) Lah, M. S.; Pecoraro, V. L. *J. Am. Chem. Soc.* **1989**, *111*, 7258.

(21) Mezei, G.; Zaleski, C. M.; Pecoraro, V. L. *Chem. Rev.* **2007**, *107*, 4933.

(22) Moon, D.; Song, J.; Kim, B. J.; Suh, B. J.; Lah, M. S. *Inorg. Chem.* **2004**, *43*, 8230.

(23) Boron, T. T.; Kampf, J. W.; Pecoraro, V. L. *Inorg. Chem.* **2010**, *49*, 9104.

(24) Cooper, M. J. *X-ray Compton Scattering*; Oxford University Press: Oxford, 2004.

(25) Koizumi, A.; Miyaki, S.; Kakutani, Y.; Koizumi, H.; Hiraoka, N.; Makoshi, K.; Sakai, N.; Hirota, K.; Murakami, Y. *Phys. Rev. Lett.* **2001**, *86*, 5589.

(26) Deb, A.; Itou, M.; Sakurai, Y.; Hiraoka, N.; Sakai, N. *Phys Rev B* **2001**, *63*, 064409.

(27) Barbiellini, B.; Koizumi, A.; Mijnarends, P. E.; Al-Sawai, W.; Lin, H.; Nagao, T.; Hirota, K.; Itou, M.; Sakurai, Y.; Bansil, A. *Phys. Rev. Lett.* **2009**, *102*, 206402.

(28) Thole, B. T.; Vanderlaan, G.; Fuggle, J. C.; Sawatzky, G. A.; Karnatak, R. C.; Esteva, J. M. *Phys. Rev. B* **1985**, *32*, 5107.

(29) Arrio, M. A.; Scuiller, A.; Sainctavit, P.; Moulin, C. C. D.; Mallah, T.; Verdaguer, M. *J. Am. Chem. Soc.* **1999**, *121*, 6414.

(30) McCarthy, J. E.; Cooper, M. J.; Lawson, P. K.; Timms, D. N.; Manninen, S. O.; Hamalainen, K.; Suortti, P. *J. Synchrotron Radiat.* **1997**, *4*, 102.

(31) Lovesey, S. W. *J. Phys.: Condens. Matter* **1996**, *8*, L353.

(32) Carra, P.; Fabrizio, M.; Santoro, G.; Thole, B. T. *Phys. Rev. B* **1996**, *53*, R5994.